Jurnal Kejuruteraan 38(5) 2026: 2239-2251
https://doi.org/10.17576/jkukm-2026-38(5)-12

High-Performance Titanium Composites: Mechanical and Metallurgical Characterization of Powder Metallurgy-Synthesized Materials

Yonaf Wakuma[a], Devendra Kumar Sinha[b,c], Abdulrahman Aljabri[d] ,Asad A. Zaidi[d,e], Gaurav Gupta[f], Muhammad Asif[g], Gulam Mohammed Sayeed Ahmed[b,c] & Sohaib Z. Khan[d*]

[a]*Department of Mechanical Engineering, College of Engineering, Wolaita Sodo University, Wolaitasodo, Ethiopia*

[b]*Department of Mechanical Engineering, Adama Science & Technology University, Adama City, Ethiopia.*

[c]*Centre of excellence (COE) for Advanced Manufacturing Engineering, Department of Mechanical Engineering, Adama Science & Technology University, Adama, 1888, Ethiopia.*

[d]*Department of Mechanical Engineering, Islamic University of Madinah, Medina 42351, Saudi Arabia.*

[e]*Sustainability Research Center, Islamic University of Madinah, Madinah, Saudi Arabia.*

[f]*AMITY Department of Mechanical Engineering, College of Engineering, Noida, India.*

[g]*Department of Engineering Sciences, PNEC, National University of Sciences and Technology, Karachi, 75350, Pakistan*

**Corresponding author: szkhan@iu.edu.sa*

Received 17 August 2025, Received in revised form 19 February 2026
Accepted 19 March 2026, Available online 30 August 2026

ABSTRACT

Titanium metal matrix composites (Ti-MMCs) are advanced materials that offer superior mechanical properties, corrosion resistance, and structural integrity, making them well-suited for high-performance applications. This study investigates the effect of reinforcement particle composition on the mechanical and metallurgical properties of Ti-MMCs. Titanium Grade 5 (Ti-6Al-4V) powder was used as the matrix material, while cerium oxide (CeO2), chromium (Cr), and graphite (Gr) were employed as reinforcements. The composites were synthesized through powder metallurgy, which involved ball milling, hydraulic compaction, and high-temperature sintering. The synthesized composites were analyzed for phase composition and microstructure using X-ray diffraction (XRD) and optical microscopy. Hardness was assessed using a Vickers hardness tester, while compressive strength was evaluated through a universal testing machine. Corrosion resistance was examined via potentiodynamic polarization testing. Among the fabricated samples, Ti-6Al-4V composite reinforced with 5% CeO_2, 10% Cr, and 4% Gr demonstrated the lowest porosity (4.37%) and the highest relative density (95%), indicating effective densification. This composition also exhibited superior mechanical properties, with a hardness of 682 HV and a compressive strength of 914 MPa. Furthermore, it provided corrosion resistance by achieving a protection efficiency of 76% and a corrosion current of 19.27 mA/cm², compared to pure Ti-6Al-4V. FT-IR analysis confirmed the presence of Ti-6Al-4V–O bonding and the absence of hydroxyl absorption bands, indicating enhanced corrosion resistance. These findings highlight the potential of Ti-MMCs for biomedical applications, particularly in orthopedic implants requiring high strength, durability, and corrosion resistance. The study demonstrated that hybrid reinforcement tailoring is a viable strategy for engineering multifunctional Ti-based composites.

Keywords: Powder metallurgy; titanium metal matrix composites; vickers hardness; SEM; Corrosion

INTRODUCTION

Metal Matrix Composites (MMCs) are engineered materials designed to enhance mechanical, thermal, and corrosion-resistant properties by incorporating reinforcements into a metallic matrix (Tang et al. 2025). Among various MMCs, titanium-based composites (Ti-MMCs) have emerged as promising materials due to their exceptional strength-to-weight ratio, high-temperature stability, and superior biocompatibility (Torghabeh and Pouriamanesh, 2022). These properties make Ti-MMCs suitable for applications in aerospace, biomedical implants, and high-performance structural components. However, titanium alloys, such as Ti-6Al-4V, suffer from inherent drawbacks, including poor wear resistance, high production costs, and difficulties in machining (Ammisetti and Harish Kruthiventi, 2021; Shetty et al. 2022). To address these limitations, reinforcing titanium with ceramic and metallic particles, such as cerium oxide (CeO_2) and chromium (Cr), has been explored to enhance mechanical strength, wear resistance, and corrosion protection (Fallah barzoki et al. 2022).

Ti-MMCs typically consist of a titanium alloy matrix reinforced with ceramic or metallic particles, which improve both mechanical and tribological properties. Reinforcements such as TiB_2, TiC, and SiC have been widely studied for their ability to enhance the hardness and wear resistance of titanium alloys (Zhai et al. 2022). These reinforcement phases act as load-bearing constituents that prevent dislocation movement, thereby improving the composite's strength and stiffness (Bagheri et al. 2021). Ti-6Al-4V, the most commonly used titanium alloy, has been reinforced with various ceramic particles through techniques such as spark plasma sintering (Ogunmefun et al. 2023) and hot pressing (Rominiyi and Mashinini, 2023). While these methods have demonstrated improvements in hardness and strength, challenges such as interfacial bonding and porosity remain significant concerns.

Powder metallurgy has emerged as a viable technique for producing Ti-MMCs, offering advantages such as near-net shape manufacturing, controlled microstructural evolution, and reduced material wastage (Mas'ood et al. 2018; Miracle, 2005). This study explores the use of CeO_2 and Cr as reinforcements in Ti-MMCs fabricated through powder metallurgy to optimize mechanical and corrosion properties.

Cerium oxide (CeO_2) has been widely studied for its role in enhancing oxidation resistance, tribological behavior, and microstructural stability in metal matrix composites (Anand Babu et al. 2022). The incorporation of CeO_2 in Ti-MMCs has been found to improve wear resistance and reduce thermal expansion, making it a potential candidate for high-performance applications (Nemati et al. 2022). Additionally, CeO_2 has been shown to enhance the formation of passivation layers in titanium alloys, thereby increasing their corrosion resistance (Mendez et al. 2022). Research by Chenliang Chu et al. (Chu et al. 2021) demonstrated that CeO_2 doping in Fe-based coatings significantly reduced thermal conductivity and enhanced oxidation resistance, further supporting its application in Ti-MMCs.

Chromium (Cr) is another reinforcement material that enhances the mechanical properties of MMCs. Studies have shown that Cr can increase hardness, improve fracture toughness, and enhance wear resistance by forming intermetallic compounds with titanium (Ding et al. 2016; Wang et al. 2023). Chromium-based reinforcements have also been reported to improve corrosion resistance by promoting the formation of stable passivation layers (Ning et al. 2024; Yu et al. 2024). In a study by Mohammed et al. (Mohammed et al. 2018), the addition of Cr_2O_3 nanoparticles significantly enhanced the tensile strength and hardness of aluminum-based composites. Similarly, Li et al (Li et al. 2019) observed that Cr_3C_2-reinforced Ti-MMCs exhibited superior compressive strength and phase stability.

Powder metallurgy has been recognized as an effective technique for producing metal matrix composites with improved uniformity and enhanced properties (Manjunath et al. 2021). Compared to conventional casting techniques, powder metallurgy ensures better control over reinforcement distribution, reduces material defects, and enables the fabrication of complex geometries (Das et al. 2022). The fabrication process typically involves mechanical mixing of matrix and reinforcement powders, followed by compaction and sintering under controlled temperature conditions (Gupta et al. 2022). Sintering plays a crucial role in promoting diffusion bonding between the matrix and reinforcement phases, thereby influencing the final composite properties (Lv et al. 2025).

Recent advancements in powder metallurgy have led to the development of hybrid Ti-MMCs reinforced with multiple ceramic and metallic constituents to achieve optimized mechanical and corrosion properties (Ammisetti et al. 2024). Studies by Ghodrati & Ghomashchi (Ghodrati and Ghomashchi 2019) indicate that graphene, when combined with CeO_2 and Cr, enhances interfacial bonding and wear resistance, making Ti-MMCs more suitable for extreme operating conditions. However, achieving uniform dispersion of reinforcement particles remains a significant challenge, often requiring high-energy ball milling to ensure homogeneity (Sui et al. 2024).

This study aims to develop and characterize Ti-MMCs reinforced with CeO_2 and Cr using the powder metallurgy approach. The primary research objectives include:

1. Fabrication of Ti-6Al-4V-based composites with varying reinforcement concentrations using powder metallurgy techniques.
2. Microstructural and phase characterization using X-ray diffraction (XRD), scanning electron microscopy (SEM), and optical microscopy.
3. Evaluation of mechanical properties, including hardness and compressive strength, to assess the effectiveness of CeO_2 and Cr reinforcements.
4. Assessment of corrosion resistance using electrochemical techniques to determine the effect of reinforcement materials on passivation behavior.
   a.

By integrating CeO_2 and Cr reinforcements into Ti-MMCs, this study seeks to develop high-performance composites with enhanced hardness, corrosion resistance, and structural integrity. The findings will contribute to the advancement of titanium-based materials for aerospace, biomedical, and industrial applications.

MATERIALS AND METHODS

MATERIAL SELECTION AND PREPARATION

This study investigates the mechanical and metallurgical characteristics of titanium metal matrix composites (Ti-MMCs) reinforced with cerium oxide (CeO_2) and chromium (Cr) particles. The base material used for the composite matrix is Titanium Ti-6Al-4V, a widely used titanium alloy known for its high strength, corrosion resistance, and biocompatibility. The reinforcement materials include CeO_2, which is selected for its superior corrosion resistance, thermal stability, and its ability to enhance passivation layer formation (Jiang et al. 2020). Cr is Chosen for its contribution to hardness, wear resistance, and the formation of stable intermetallic phases in Ti-MMCs (Wang et al. 2023), and Gr is incorporated to enhance self-lubrication and reduce friction in tribological applications (Huebner and Young, 2013). Ti-6Al-4V powder was used as the primary matrix material due to its excellent mechanical properties and corrosion resistance (Hu et al. 2021). Figure 1 shows the morphology of the Ti-6Al-4V powder used in this study. CeO_2 powder was used as a reinforcement material to enhance corrosion resistance and thermal stability (Chen et al. 2021). The powder was characterized by a fine particle size distribution (see Figure 2), ensuring uniform dispersion within the matrix. Chromium was selected due to its known contributions to wear resistance and microstructural stability (Mohammed et al. 2018). Graphite was introduced to improve the lubrication properties of Ti-MMCs (Wang, 2013). The visual morphology of Cr and graphite powder is presented in Figure 3, purchased from Parshwamani Metals, Mumbai, India. Table 1 presents the mechanical properties of Ti-6Al-4V, CeO_2, Cr, and graphite, sourced from the MiT Database**.**

TABLE 1. Mechanical properties of Titanium Ti-6Al-4V from MiT Database

Mechanical Properties	Titanium Ti-6Al-4V	CeO_2	Cr	Graphite Powder
Compressive strength (MPa)	848 - 1080	590	282	14
Elastic modulus (GPa)	110 - 119	180	140	11.5
Hardness (Mohs)	6.5	6.5	8.5	-
Density (g/cm^3)	4.43 - 4.51	7.13	7.15	2.26
Thermal conductivity (W/mK)	0.8	0.8	69.1	200
Melting point (^{o}C)	2400	2400	1907	3600
Poisson's Ratio	0.31-0.37	0.28	0.21	-
Heat Capacity (J/gk)	-	-	-	720

FIGURE 1. Titanium Ti-6AL-4V powder

FIGURE 2. Cerium oxide (CeO2) powder

(a) (b)

FIGURE 3. (a) Chromium (Cr) powder and (b) Graphite powder

POWDER METALLURGY PROCESS

The Ti-6Al-4V matrix powder was mixed with varying weight fractions of CeO_2, Cr, and graphite using a high-energy ball milling machine (Figure 4). The milling process aimed to achieve uniform distribution of the reinforcements while reducing particle size and agglomeration. Milling parameters were as follows: milling speed, 200 rpm; milling time, 2 hours; ball diameter, 10 mm; ball-to-powder weight ratio, 10:1; and milling temperature, room temperature.

After milling, the mixed powder was compacted using a 25-ton hydraulic press machine to form cylindrical green compacts (Figure 5). The compaction was performed using a uniaxial pressing technique, ensuring homogeneous density distribution. Compaction parameters included applied pressures of 0 MPa, 15 MPa, and 40 MPa, a holding time of 60 minutes, and die and punch specifications with pre-designed dimensions provided in Table 2.

TABLE 2. The die and punch dimensions

S. No	Parameters of the die and punch	Dimension, mm
1	Outer diameter of the die	50
2	Inner diameter of the die	20
3	Length of the die	50
4	Diameter of the punch	20- clearance
5	Length of the punch	50

FIGURE 4. High-energy ball milling machine for powder mixing process and powder compaction

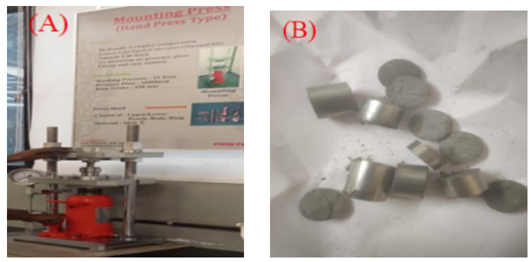

FIGURE 5. Photos of (A) Mounting Press set up and (B) Compacted Specimen (Green Part)

The green compacts were sintered at 1100°C for 2 hours in a controlled argon atmosphere to prevent oxidation and promote diffusion bonding between matrix and reinforcements (Tong, 2011). The sintering process involved a gradual heating rate of 10°C/min with an argon gas flow rate of 10 L/min (Figure 6). Sintering was carried out in three stages: (1) Initial Stage: Formation of particle necks with minimal densification. (2) Intermediate Stage: Growth of necks, reduction of porosity, and grain recrystallization. (3) Final Stage: Grain coarsening and elimination of remaining voids (Das et al. 2022).

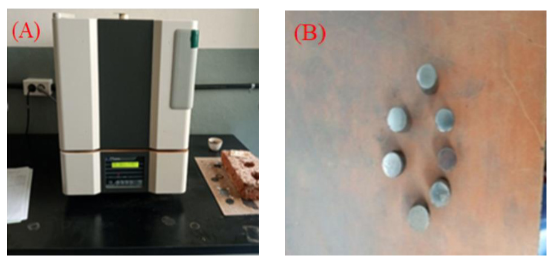

FIGURE 6. (A) The Furnace Set Up and (B) The Sintered Samples

SPECIMEN PREPARATION FOR CHARACTERIZATION

After sintering, specimens were prepared for microstructural, mechanical, and corrosion analysis using standard metallographic techniques (Figure 7). The steps included (1) Cutting and Sectioning: A hand saw and file were used for sample preparation. (2) Mounting: Hot compression mounting was performed to maintain sample integrity. (3) Grinding and Polishing: Progressive grinding with 120-2000 grit SiC paper, followed by polishing with a diamond suspension. (4) Etching: Samples were etched using a solution of methanol, HCl, HNO_3, and HF for microstructural analysis.

FIGURE 7. Sample Preparation

DESIGN OF EXPERIMENT FOR TI-MMC FABRICATION

A total of four Ti-6Al-4V-based metal matrix composites (Ti-MMCs) were synthesized using the powder metallurgy technique, with varying weight percentages of cerium oxide (CeO_2) and chromium (Cr) reinforcements. Graphite (Gr) was added as a solid lubricant at a constant concentration of 4 wt% in all composite samples. One unreinforced sample (S4) was also fabricated as a control. The objective was to examine how different combinations of CeO_2 and Cr affect the physical, mechanical, and corrosion properties of the Ti-MMCs. The sample compositions are listed in Table 3.

TABLE 3. The die and punch dimensions

Sample Code	Ti-6Al-4V (wt%)	CeO_2 (wt%)	Cr (wt%)	Graphite (wt%)
S1	81	5	10	4
S2	81	10	5	4
S3	81	7.5	7.5	4
S4 (Control)	100	0	0	0

This experimental matrix was developed based on findings from previous studies (Gupta et al. 2022; Yu and Guo, 2019), where CeO_2 and Cr have demonstrated significant potential to enhance the wear resistance, mechanical performance, and corrosion behavior of metal matrix systems. A hybrid reinforcement strategy was adopted to investigate the potential synergistic effects between ceramic (CeO_2) and metallic (Cr) constituents. Each sample was compacted using a 25-ton hydraulic press and sintered under identical conditions to ensure a consistent fabrication baseline.

EXPERIMENTAL PROCEDURE

The theoretical density ($\rho_{theoretical}$) was calculated using the rule of mixtures, incorporating the densities and volume fractions of Ti-6Al-4V, CeO_2, Cr, and graphite. The experimental (sintered) density (ρ_{actual}) was measured using Archimedes' principle:

$$\rho_{actual} = \frac{W_{air}}{W_{air} - W_{water}} \tag{1}$$

Where:
W_{air} = Weight in air
W_{water} = Weight suspended in water
Porosity (%) was calculated using the following expression:

$$Porosity = \left(\frac{\rho_{theoratical} - \rho_{actual}}{\rho_{theoratical}}\right) \times 100 \tag{2}$$

This methodology aligns with that used in recent powder metallurgy studies (Zegeye et al. 2021).

Hardness was measured using a Vickers hardness tester with the following parameters: Load: 10 kgf; Dwell Time: 5 seconds; Specimen Dimensions: Cylindrical samples (Ø = 18 mm, height = 7 mm), polished with SiC papers (grit 120 to 800). Three indentations were taken per sample, and the average hardness value was reported.

Compression testing was performed using a universal testing machine (UTM) with a capacity of 50 kN in accordance with ASTM E9. Specimen geometry: Diameter: 6 mm; Length: 18 mm (length-to-diameter ratio = 3). Compressive strength was calculated from the maximum load (*F*) divided by the cross-sectional area (A):

$$\sigma_{compressive} = \frac{F}{A} \tag{3}$$

Samples were sectioned, ground, polished, and etched using a solution composed of 25 mL methanol, 25 mL hydrochloric acid, 25 mL nitric acid, and one drop of hydrofluoric acid. Optical microscopy (OM) was performed using a Huvitz HR-300 microscope to examine grain morphology and dispersion of reinforcement. Scanning Electron Microscopy (SEM) was employed to analyze fracture surfaces (fractography), observe particle clustering and porosity, and map the distribution of reinforcement.

XRD analysis was conducted using a Shimadzu XRD-7000 Maxima diffractometer with Cu-Kα radiation. Scanning parameters: Voltage: 40 kV; Current: 30 mA; Range: 10° to 80° 2θ; Step size: 3°/min. Microstructural parameters such as crystallite size, lattice strain, and dislocation density were calculated using peak broadening analysis and the Scherrer equation:

$$D = \frac{K\lambda}{\beta Cos\theta} \qquad (4)$$

Potentiodynamic polarization tests were conducted in a 3.5% NaCl solution using a standard three-electrode electrochemical cell. The corrosion parameters—including: Corrosion current density (Icorr); Corrosion potential (Ecorr); Protection efficiency (ηp); —were obtained using Tafel extrapolation and analyzed using OriginPro software. Protection efficiency was calculated as:

$$\eta_p = \left(\frac{T_{corr,bare} - I_{corr,sample}}{I_{corr,bare}}\right) \times 100 \qquad (5)$$

Where:
$I_{corr,\ bare}$ = corrosion current of pure Ti-6Al-4V
$I_{corr,\ sample}$ = corrosion current of composite

RESULTS AND DISCUSSION

ANALYSIS OF DENSITY AND POROSITY OF SINTERED SAMPLES

The densification and porosity of the sintered Ti-MMCs are key indicators of microstructural integrity, mechanical performance, and the success of the powder metallurgy process. Theoretical densities were calculated using the rule of mixtures based on the component materials' densities, while actual (sintered) densities were measured using Archimedes' principle. The relative density, which reflects the effectiveness of sintering and compactability, was calculated from these values. Results are presented in Table 4 and visualized in Figure 8.

TABLE 4. Experimental Density, Relative Density and Porosity

Sample	Theoretical Density (g/cm^3)	Sintered Density (g/cm^3)	Relative Density (%)	Porosity (%)
S1	4.8345	4.619	95.56	4.44
S2	4.8575	4.396	90.5	9.5
S3	4.8461	4.351	89.8	10.2
S4	4.5125	4.291	95.09	4.91

Among all compositions, Sample S1 demonstrated the highest relative density and the lowest porosity, indicating superior densification and minimal void formation. The optimized reinforcement ratio in S1 (5% CeO_2 and 10% Cr) promoted efficient packing and sintering due to synergistic interactions between particles. In contrast, S3, which had equal Cr and CeO_2 content (7.5% each), showed the highest porosity (10.2%), attributed to agglomeration and inhomogeneous particle dispersion that interfered with compact formation. This aligns with prior observations by Zegeye et al (Zegeye et al. 2024) and Gong et al. (Gong et al. 2025), who noted that uneven distribution of reinforcement particles during compaction can lead to microvoids and lower effective densification. Lower porosity is crucial for enhanced mechanical integrity and wear resistance; the importance of optimizing reinforcement ratios.

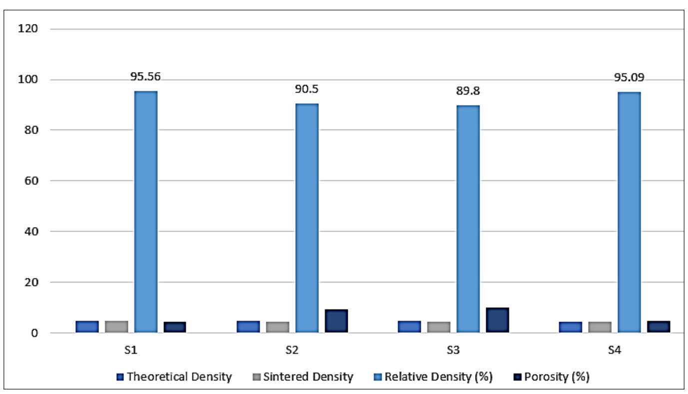

FIGURE 8. Physical Properties of Sintered Samples

HARDNESS TEST

The surface hardness of the composite samples was evaluated using Vickers hardness testing. The results are summarized in Table 5 and visualized in Figure 9. Sample S1 displayed the highest hardness value of 682 HV, followed by S2 (650 HV), S3 (616 HV), and the unreinforced alloy S4 (390 HV).

TABLE 5. Experimental Results of Hardness Values

Samples	Experimental Results of Hardness Value (HV)				
	Trial 1	Trial 2	Trial 3	Average (HV)	Improvement (%)
S1	675.4	680.3	690.3	682	75
S2	636.2	646.5	667.3	650	67
S3	604.2	619.2	624.6	616	58.46
S4	389.2	389.3	391.5	390	0

The marked increase in hardness, particularly in S1, is a result of the reinforcing effect of hard Cr particles and the grain boundary strengthening facilitated by CeO_2 particles. Chromium's high Mohs hardness contributes to dislocation pinning and wear resistance. CeO_2, on the other hand, promotes fine-grain formation and acts as a dispersion strengthener. The reduced hardness in S3 compared to S1, despite similar reinforcement totals, highlights the role of reinforcement distribution. S3's higher porosity and potential for particle agglomeration limited its surface strengthening effect.

The hardness trends closely correlate with the densification behavior observed in Section 5.1, as lower porosity in samples like S1 and S2 resulted in more effective load transfer and higher surface hardness.

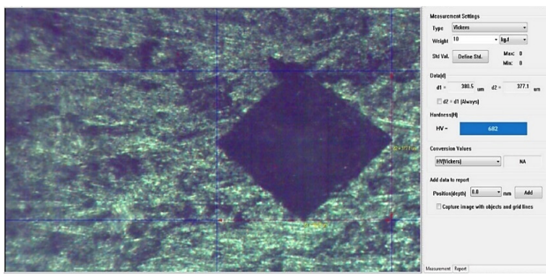

FIGURE 9. Vickers Hardness value trial for (Ti-6Al-4v)-CeO2/ Cr Composite

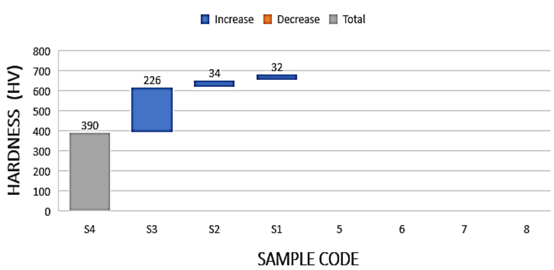

FIGURE 10. Hardness of Titanium and Composite

COMPRESSION TEST

The compressive strength of Ti-MMCs is a critical indicator of their load-bearing capacity, particularly for biomedical and structural applications. The stress-strain behavior is illustrated in Figure 11.

Sample S1 again outperformed other compositions with a compressive strength of 914 MPa. This strength enhancement is attributed to a combination of factors, including the high load-bearing capacity of Cr particles, reduced porosity, and the uniform load distribution due to good reinforcement dispersion. Sample S2 followed closely with 889 MPa, suggesting that CeO_2 also contributes significantly to matrix strengthening, likely by inhibiting crack propagation and enhancing dislocation density. The lower strengths of S3 (842 MPa) and S4 (791 MPa) confirm the adverse effects of porosity and the absence of reinforcements, respectively. These trends align with studies by Chen et al. (Chen et al. 2022), who highlighted the role of reinforcement synergy and distribution in achieving optimal compressive strength in MMCs.

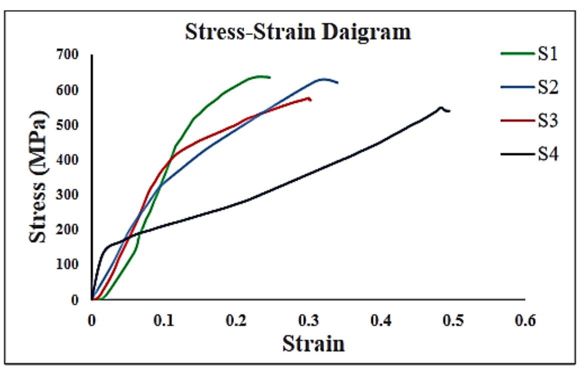

Figure 4.9 Stress- Strain Diagram of (S1, S2, S3, And S4)

FIGURE 11. Stress-strain curves for different samples (S1, S2, S3 and S4)

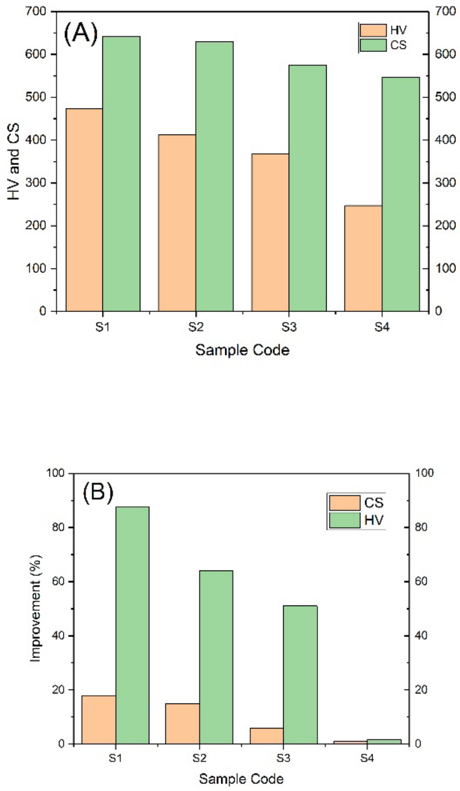

FIGURE 12. (a) Average Vickers Hardness and Compressive Strength and (b) Improvement Recorded

These strength results align well with the hardness and porosity data, confirming that lower porosity and better reinforcement bonding contribute to enhanced mechanical performance.

FRACTURE ANALYSIS USING SEM

The fracture behavior of selected samples (S2 and S3) was further analyzed using scanning electron microscopy to understand failure mechanisms. The SEM micrographs are shown in Figure 13.

Sample S2 exhibited ductile features, such as dimpled fracture surfaces, indicating plastic deformation and energy absorption prior to failure. These features suggest that the reinforcements are effective in load transfer and crack arrest. In contrast, Sample S3 exhibited brittle fracture characteristics, including cleavage planes and intergranular fracture. The presence of microvoids and interfacial debonding confirms poor bonding and higher porosity, reinforcing the earlier results from density and compression analyses. These observations align with findings from Hill et al. (Hill et al. 2011), who reported that well-bonded, uniformly dispersed reinforcements act as crack arresters and enhance the toughness of MMCs.

The brittle fracture observed in S3 is consistent with its higher porosity and lower hardness, while the ductile behavior in S1 and S2 reflects their improved densification and reinforcement distribution.

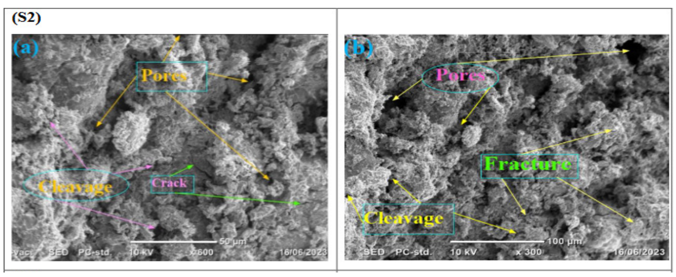

(a) (b)

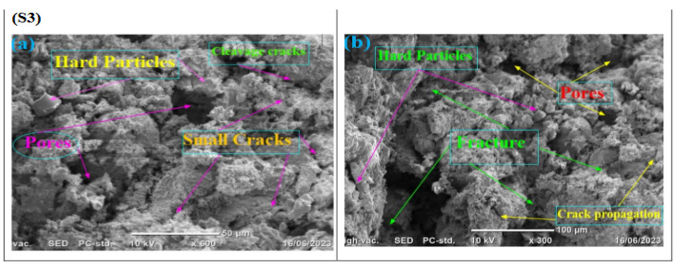

(c) (d)

FIGURE 13. (a), (b), (c), (d): Fractography Analysis Using SEM for (S2) and (S3) at 50 µm and 100µm

POTENTIODYNAMIC POLARIZATION AND CORROSION BEHAVIOR

Corrosion resistance is a critical parameter for materials used in biomedical and marine applications. Potentiodynamic polarization studies were conducted in a 3.5% NaCl solution, utilizing Tafel extrapolation to determine the corrosion current (Icorr), corrosion potential (Ecorr), and protection efficiency. The results are presented in Table 6 and illustrated in Figure 14.

TABLE 6. Tafel Polarization Experimental Parameters Values

Samples	Icorr (mA/cm^2)	Ecorr (mV)	βa (mV)	βc (mV)	RP (Ω)	CR (mm/yr)	μ_p (%)
S1	2.51	-157.91	11.06	21.48	16.45	0.34	76.55
S2	3.57	-161.85	17.07	23.34	15.6	0.51	66.5
S3	3.68	-160.2	14.24	39.01	16.05	0.54	65.1
S4	7.245	-182.04	12.6	39.94	7.53	1.090	32.5
Pure Ti-6Al-4V	10.5	-246.94	7.21	45.68	3.34	1.34	0.00

The corrosion results followed the same trend observed in mechanical properties, with Sample S1 demonstrating the best performance. Its low Icorr and high Ecorr indicate stable passive layer formation and resistance to chloride-induced pitting. The addition of Cr is known to facilitate the formation of a dense, adherent oxide film that protects against further oxidation. Meanwhile, CeO_2 enhances corrosion resistance by scavenging oxygen and forming barrier layers that block aggressive Cl^- ions (Mendez et al. 2022). These synergistic effects are less pronounced in S3 due to its compromised microstructure, as confirmed by its higher porosity and tendency towards microcracking.

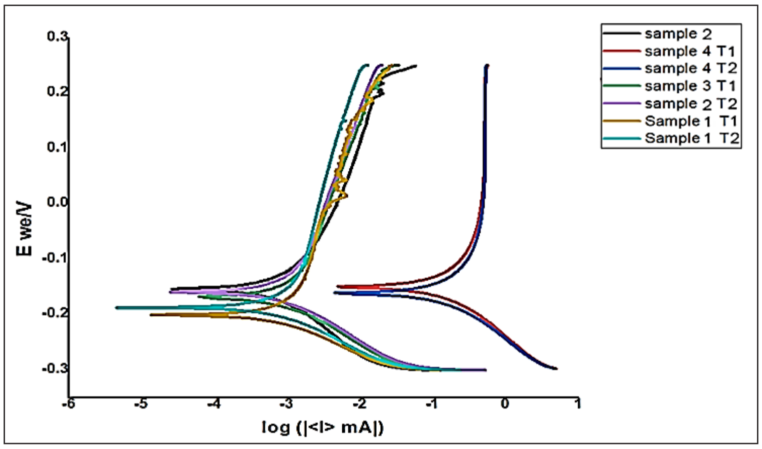

FIGURE 14. The Tafel Polarization Plot of Titanium and Ti-MMC's

The corrosion resistance trend also correlates with the microstructure and porosity, where lower porosity and uniform dispersion of reinforcements in S1 limited electrolyte penetration and improved protection efficiency.

SEM ANALYSIS OF REINFORCEMENT DISTRIBUTION

To assess reinforcement dispersion and matrix homogeneity, SEM micrographs were taken at different magnifications for all samples. Figure 15 illustrates the microstructural quality and distribution of CeO_2 and Cr particles within the Ti-6Al-4V matrix.

Sample S1 exhibited a uniform dispersion of CeO_2 and Cr particles, minimal porosity, and no significant agglomeration, which supports its superior mechanical and corrosion properties. Sample S2 exhibited slightly uneven dispersion, with localized clustering. Sample S3 showed clear signs of reinforcement agglomeration and pore clustering, validating its inferior mechanical and corrosion performance. The control sample S4, with no reinforcements, showed larger grains and higher porosity, which negatively impacted its strength and corrosion resistance. These micrographs confirm

that uniform dispersion of hybrid reinforcements is key to enhancing the structural integrity of Ti-MMCs.

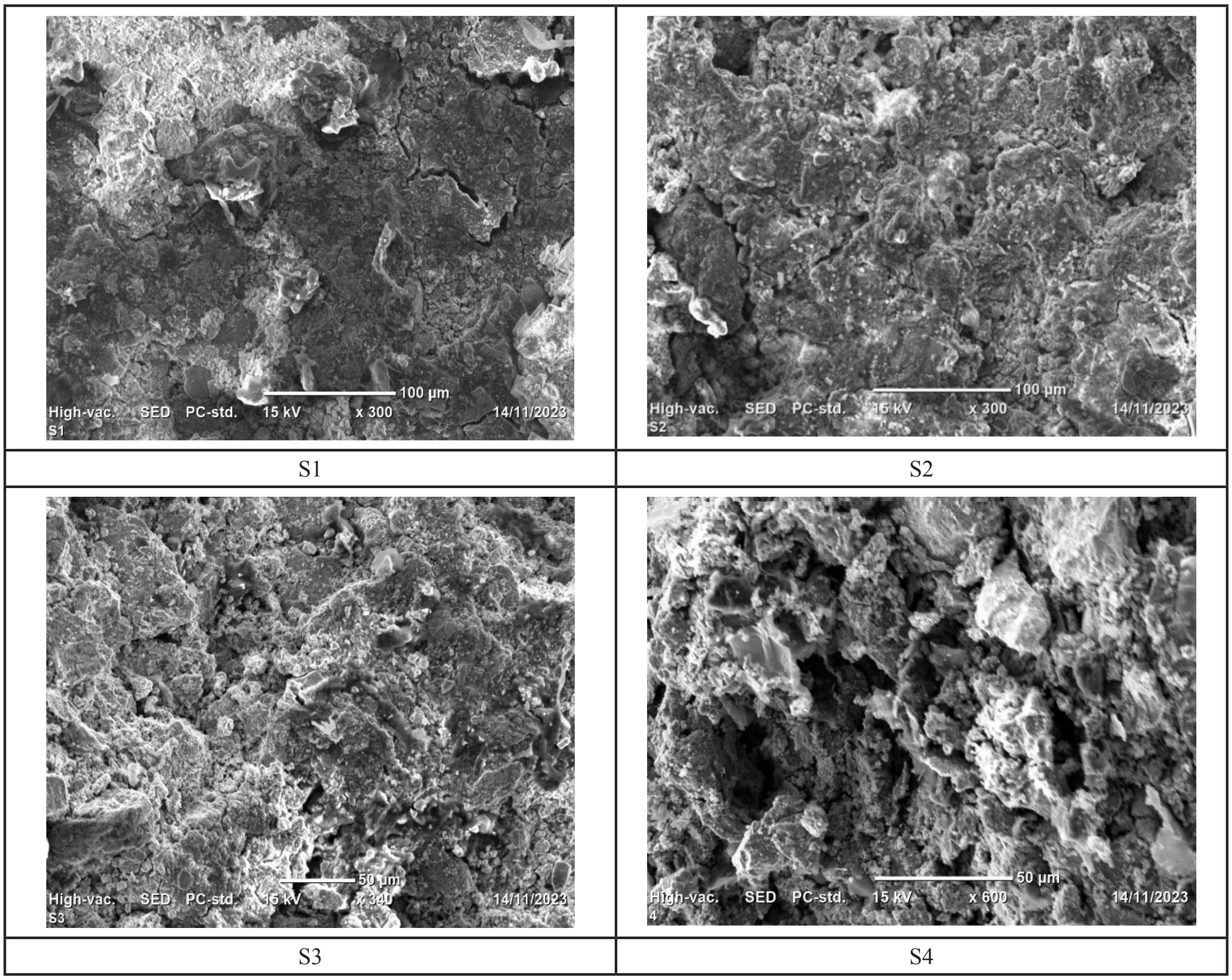

FIGURE 15. SEM Micrographs of (S1, S2, S3 And S4) at Different Magnification showing surface morphology and reinforcement dispersion. Due to the absence of EDX analysis, individual reinforcement phases such as Cr and CeO_2 could not be distinctly identified; however, microstructural differences in particle dispersion and porosity are visually evident across the samples

CONCLUSION

This study successfully demonstrated the fabrication and comprehensive characterization of titanium metal matrix composites (Ti-MMCs) reinforced with cerium oxide (CeO_2), chromium (Cr), and graphite (Gr) via powder metallurgy. Four distinct compositions were synthesized and systematically evaluated for their physical, mechanical, and corrosion properties.

Among all samples, the composite with 5 wt% CeO_2, 10 wt% Cr, and 4 wt% Gr (Sample S1) consistently exhibited superior performance. It achieved the highest relative density (95.56%), hardness (682 HV), and compressive strength (914 MPa), while also displaying the lowest porosity (4.44%) and the best corrosion resistance (protection efficiency of 76.55%). The reinforcement distribution in S1 was found to be uniform, with minimal agglomeration or porosity, as evidenced by SEM analysis.

The results emphasize the importance of optimizing the type and proportion of reinforcement particles. Chromium contributed significantly to mechanical enhancement through solid-solution strengthening and load transfer, while CeO_2 improved corrosion resistance by stabilizing the passive oxide film and inhibiting chloride ion attack. Graphite, used as a solid lubricant, supported overall structural stability without compromising mechanical strength.

The study confirmed that powder metallurgy is an effective method for producing high-performance Ti-MMCs with controlled microstructures and enhanced multi-functional properties. Future work may focus on tailoring processing parameters, such as milling time, sintering profile, and reinforcement morphology, to refine composite performance further.

These findings have significant implications for applications in biomedical implants, aerospace, and structural components, where a high strength-to-weight ratio, corrosion resistance, and durability are critical. The combination of CeO_2 and Cr as hybrid reinforcements presents a promising pathway for engineering next-generation titanium-based composites.

ACKNOWLEDGEMENT

During the preparation of this work, the authors used ChatGPT 4.0 to refine writing and improve readability. The authors have reviewed and edited the AI-generated content as necessary and take full responsibility for the contents of this publication

DECLARATION OF COMPETING INTEREST

None.

REFERENCES

Ammisetti, D. K. & Harish Kruthiventi, S. S. 2021. Recent trends on titanium metal matrix composites: A review. *Materials Today: Proceedings* 46: 9730–9735. https://doi.org/10.1016/j.matpr.2020.08.732

Ammisetti, D. K., Kruthiventi, S. S. H., Vinjavarapu, S., Babu, N. N., Gandepudi, J. R. & Battula, S. K. 2024. A review on reinforcements, fabrication methods, and mechanical and wear properties of titanium metal matrix composites. *Journal of Engineering and Applied Science* 71: 60. https://doi.org/10.1186/s44147-024-00392-z

Anand Babu, V., Kumaravel, A. & Manikandan, R. 2022. Microstructure, mechanical and wear characteristics of CeO2-Mg metal matrix composites. *Proceedings of the Institution of Mechanical Engineers, Part E: Journal of Process Mechanical Engineering* 237: 430–440. https://doi.org/10.1177/09544089221139592

Bagheri, S., Khalil, I. & Julkapli, N. M. 2021. Cerium(IV) oxide nanocomposites: Catalytic properties and industrial application. *Journal of Rare Earths* 39: 129–139. https://doi.org/10.1016/j.jre.2020.02.022

Chen, F., Mei, Q. S., Li, J. Y., Li, C. L., Wan, L., Mei, X. M., Chen, Z. H., Xu, T., Wang, Y. C. & Tan, Y. Y. 2022. Achieving synergistic strengthening and enhanced comprehensive properties of Cu matrix composites at high strength level by incorporating nanocarbons and Al2O3 dual reinforcements. *Materials Science and Engineering A* 839: 142859. https://doi.org/10.1016/j.msea.2022.142859

Chen, L., Zhao, Y., Guan, C. & Yu, T. 2021. Effects of CeO2 addition on microstructure and properties of ceramics reinforced Fe-based coatings by laser cladding. *International Journal of Advanced Manufacturing Technology* 115: 2581–2593. https://doi.org/10.1007/s00170-021-07297-8

Chu, C., Chen, W., Chen, Z., Jiang, Z., Wang, H. & Fu, Z. 2021. Microstructure and mechanical behavior of FeNiCoCr and FeNiCoCrMn high-entropy alloys fabricated by powder metallurgy. *Acta Metallurgica Sinica (English Letters)* 34: 445–454. https://doi.org/10.1007/s40195-020-01150-9

Das, R., Mondal, M. K. & Pramanik, S. 2022. Strengthening behaviour and microstructural properties during the compaction of reduced blast furnace flue dust–fly ash–iron metal matrix composite fines using powder metallurgy route. *Transactions of the Indian Institute of Metals* 75: 2255–2263. https://doi.org/10.1007/s12666-022-02592-8

Ding, H., Liu, S., Zhang, H. & Guo, J. 2016. Improving impact toughness of a high chromium cast iron regarding joint additive of nitrogen and titanium. *Materials & Design* 90: 958–968. https://doi.org/10.1016/j.matdes.2015.11.055

Fallah Barzoki, M., Fatemi, S. & Ganjali, M. R. 2022. Fabrication and comparison of composites of cerium metal-organic framework/reduced graphene oxide as the electrode in supercapacitor application. *Journal of Energy Storage* 55: 105545. https://doi.org/10.1016/j.est.2022.105545

Ghodrati, H. & Ghomashchi, R. 2019. Effect of graphene dispersion and interfacial bonding on the mechanical properties of metal matrix composites: An overview. *FlatChem* 16: 100113. https://doi.org/10.1016/j.flatc.2019.100113

Gong, C., Jiang, J., Liu, T., Zhang, R. & Xu, D. 2025. Compaction optimization of surfactant-tailored basalt-fiber WMA by improved lubrication and micro-structure formation. *Construction and Building Materials* 484: 141905. https://doi.org/10.1016/j.conbuildmat.2025.141905

Gupta, P., Ahamad, N., Kumar, D., Gupta, N., Chaudhary, V., Gupta, S., Khanna, V. & Chaudhary, V. 2022. Synergetic effect of CeO2 doping on structural and tribological behavior of Fe-Al2O3 metal matrix nanocomposites. *ECS Journal of Solid State Science and Technology* 11: 117001. https://doi.org/10.1149/2162-8777/ac9c92

Hill, H., Weber, S., Siebert, S. & Theisen, W. 2011. Investigation of corrosion and wear properties of Fe based metal matrix composites consolidated by sintering and hot isostatic pressing. *Powder Metallurgy* 54: 455–462. https://doi.org/10.1179/003258910X12678035166656

Hu, L., Song, X., Zhao, X., Guo, F., Yang, F. & Xiao, P. 2021. A robust, hydrophobic CeO2/NiCoCrAlY composite coating with excellent thermal stability and corrosion resistance prepared by air plasma spray. *Journal of Alloys and Compounds* 861: 158623. https://doi.org/10.1016/j.jallcom.2021.158623

Huebner, M. & Young, L. A. 2013. Materials for mechanical seals. In *Encyclopedia of Tribology*, edited by Wang, Q. J. & Chung, Y.-W., 2173–2184. Boston, MA: Springer US. https://doi.org/10.1007/978-0-387-92897-5_126

Jiang, P.-F., Zhang, C.-H., Wu, C.-L., Zhang, S., Zhang, J.-B. & Abdullah, A. O. 2020. Microstructure and properties of CeO2-modified FeCoCrAlNiTi high-entropy alloy coatings by laser surface alloying. *Journal of Materials Engineering and Performance* 29: 1346–1355. https://doi.org/10.1007/s11665-020-04621-3

Li, Y., Li, C., Tang, S., Zheng, Q., Wang, J., Zhang, Z. & Wang, Z. 2019. Interfacial bonding and abrasive wear behavior of iron matrix composite reinforced by ceramic particles. *Materials* 12(22): 3646. https://doi.org/10.3390/ma12223646

Lv, W., Lv, J., Liu, B., Zheng, Z., Mou, Y., He, S., Liu, J., Chen, C. & Kang, Y. 2025. Strategy for achieving high sintering and mechanical response performance of nano-Cu/two-dimensional material composite via nanoscale surface-defect-induced longitudinal diffusion. *Applied Surface Science* 690: 162630. https://doi.org/10.1016/j.apsusc.2025.162630

Manjunath, R., Kumar, D. & Kumar, A. 2021. A review on the significance of hybrid particulate reinforcements on the mechanical and tribological properties of stir-casted aluminum metal matrix composites. *Journal of Bio- and Tribo-Corrosion* 7: 122. https://doi.org/10.1007/s40735-021-00558-9

Mas'ood, N. N., Foudzi, F. M., Sulong, A. B., Muhamad, N., Mohamed, I. F., Salleh, F. M. & Emeka, U. B. 2018. Two component materials in powder metallurgy: A review paper focused on the processing technique applied in powder metallurgy. *Jurnal Kejuruteraan* Special Issue 1: 1.

Mendez, J. A. C., Vong, Y. M. & Bueno, J. de J. P. 2022. Cerium and other rare earth salts as corrosion inhibitors: A review. *Protection of Metals and Physical Chemistry of Surfaces* 58: 801–810. https://doi.org/10.1134/S2070205122040141

Miracle, D. B. 2005. Metal matrix composites: From science to technological significance. *Composites Science and Technology* 65: 2526–2540. https://doi.org/10.1016/j.compscitech.2005.05.027

Mohammed, H., Penchal Reddy, M., Ubaid, F., Shakoor, A. & Mohamed Amer Mohamed, A. 2018. Structural and mechanical properties of CeO2 reinforced Al matrix nanocomposites. *Advanced Materials Letters* 9: 602–605. https://doi.org/10.5185/amlett.2018.2030

Nemati, F., Rezaie, M., Tabesh, H., Eid, K., Xu, G., Ganjali, M. R., Hosseini, M., Karaman, C., Erk, N., Show, P.-L., Zare, N. & Karimi-Maleh, H. 2022. Cerium functionalized graphene nano-structures and their applications: A review. *Environmental Research* 208: 112685. https://doi.org/10.1016/j.envres.2022.112685

Ning, Y., Liu, B., Wang, Q., Wang, Z., Song, Y. & Lv, J. 2024. Oxidation control preparation of chromium-based MXene as ultrahigh performance barrier nanosheets for corrosion protection. *Corrosion Science* 235: 112184. https://doi.org/10.1016/j.corsci.2024.112184

Ogunmefun, O. A., Bayode, B. L., Jamiru, T. & Olubambi, P. A. 2023. A critical review of dispersion strengthened titanium alloy fabricated through spark plasma sintering techniques. *Journal of Alloys and Compounds* 960: 170407. https://doi.org/10.1016/j.jallcom.2023.170407

Rominiyi, A. L. & Mashinini, P. M. 2023. Spark plasma sintering of discontinuously reinforced titanium matrix composites: Densification, microstructure and mechanical properties — a review. *International Journal of Advanced Manufacturing Technology* 124: 709–736. https://doi.org/10.1007/s00170-022-10564-x

Shetty, R., Hegde, A., Shetty, S. V., U. K., Nayak, R., Naik, N. & Nayak, M. 2022. Processing and mechanical characterisation of titanium metal matrix composites: A literature review. *Journal of Composites Science* 6(12): 388. https://doi.org/10.3390/jcs6120388

Sui, X., Weng, Y., Zhang, L., Lu, J., Huang, X., Long, F. & Zhang, W. 2024. Uncovering the effect of CeO2 on the microstructure and properties of TiAl/WC coatings on titanium alloy. *Coatings* 14(5): 543. https://doi.org/10.3390/coatings14050543

Tang, J., Omar, M. Z. & Mohamed, I. F. 2025. Study on ZL205A matrix composites reinforced with in-situ TiB. *Jurnal Kejuruteraan* 37: 1553–1561.

Tong, X. C. 2011. Thermally conductive ceramic matrix composites. In *Advanced Materials for Thermal Management of Electronic Packaging*, edited by Tong, X. C., 277–304. New York, NY: Springer New York. https://doi.org/10.1007/978-1-4419-7759-5_7

Torghabeh, N. A. & Pouriamanesh, R. 2022. A review on Ti-based metal matrix composite coatings. *Journal of Composites and Compounds* 4: 209–219.

Wang, D., Lin, S., Lu, J., Huang, S., Yin, Z., Yang, H., Bian, P., Zhang, Y., Dai, M. & Zhou, K. 2023. Research on high temperature wear resistance mechanism of CrN/CrAlN multilayer coatings. *Tribology International* 180: 108184. https://doi.org/10.1016/j.triboint.2022.108184

Wang, H. 2013. Graphite solid lubrication materials. In *Encyclopedia of Tribology*, edited by Wang, Q. J. & Chung, Y.-W., 1550–1555. Boston, MA: Springer US. https://doi.org/10.1007/978-0-387-92897-5_1261

Yu, K. P., Jiang, H., Xu, X. Y. & Huang, M. X. 2024. Design of corrosion-resistant alloys for preventing oxidation-induced nanoscale Cr-depletion by inclusion engineering. *Materials & Design* 244: 113146. https://doi.org/10.1016/j.matdes.2024.113146

Yu, Y. & Guo, Y. 2019. Cerium oxide-modified lithium chromium titanate as high-performance anode material for lithium-ion battery. *Ionics* 25: 367–371. https://doi.org/10.1007/s11581-018-2758-1

Zegeye, A. D., Delele, M. A., Tsegaw, A. A. & Bogale, T. S. 2024. Characterization of the void content and laminate quality of fiber-reinforced plastic composites manufactured using the resin spray and compaction method. *Polymer Composites* 45: 1300–1315. https://doi.org/10.1002/pc.27855

Zegeye, D. B., Sinha, D. K., Venkatesh, C., Kumar, A. & Jha, P. 2021. Mathematical modeling and mechanical characterization through process parameters optimization of AlMg-matrix SiCp reinforced composites produced by powder metallurgy route. *Materials Today: Proceedings* 47: 3811–3818. https://doi.org/10.1016/j.matpr.2021.03.078

Zhai, Y., Singh, A. P., Bolzoni, L., Qu, Y., Li, Y. & Yang, F. 2022. Fabrication and characterization of in situ Ti-6Al-4V/TiB composites by the hot-pressing method using recycled metal chips. *Metals* 12(12): 2038. https://doi.org/10.3390/met12122038